NASA/TM—2006-214269

Effects of Hydrogen on GRCop-84

David L. Ellis
Glenn Research Center, Cleveland, Ohio

Keith Hastings
ERC/Jacobs Sverdrup Technology, Huntsville, Alabama

April 2006

NASA STI Program . . . in Profile

Since its founding, NASA has been dedicated to the advancement of aeronautics and space science. The NASA Scientific and Technical Information (STI) program plays a key part in helping NASA maintain this important role.

The NASA STI Program operates under the auspices of the Agency Chief Information Officer. It collects, organizes, provides for archiving, and disseminates NASA's STI. The NASA STI program provides access to the NASA Aeronautics and Space Database and its public interface, the NASA Technical Reports Server, thus providing one of the largest collections of aeronautical and space science STI in the world. Results are published in both non-NASA channels and by NASA in the NASA STI Report Series, which includes the following report types:

- TECHNICAL PUBLICATION. Reports of completed research or a major significant phase of research that present the results of NASA programs and include extensive data or theoretical analysis. Includes compilations of significant scientific and technical data and information deemed to be of continuing reference value. NASA counterpart of peer-reviewed formal professional papers but has less stringent limitations on manuscript length and extent of graphic presentations.

- TECHNICAL MEMORANDUM. Scientific and technical findings that are preliminary or of specialized interest, e.g., quick release reports, working papers, and bibliographies that contain minimal annotation. Does not contain extensive analysis.

- CONTRACTOR REPORT. Scientific and technical findings by NASA-sponsored contractors and grantees.

- CONFERENCE PUBLICATION. Collected papers from scientific and technical conferences, symposia, seminars, or other meetings sponsored or cosponsored by NASA.

- SPECIAL PUBLICATION. Scientific, technical, or historical information from NASA programs, projects, and missions, often concerned with subjects having substantial public interest.

- TECHNICAL TRANSLATION. English-language translations of foreign scientific and technical material pertinent to NASA's mission.

Specialized services also include creating custom thesauri, building customized databases, organizing and publishing research results.

For more information about the NASA STI program, see the following:

- Access the NASA STI program home page at *http://www.sti.nasa.gov*

- E-mail your question via the Internet to *help@sti.nasa.gov*

- Fax your question to the NASA STI Help Desk at 301–621–0134

- Telephone the NASA STI Help Desk at 301–621–0390

- Write to:
  NASA STI Help Desk
  NASA Center for AeroSpace Information
  7121 Standard Drive
  Hanover, MD 21076–1320

NASA/TM—2006-214269

Effects of Hydrogen on GRCop-84

David L. Ellis
Glenn Research Center, Cleveland, Ohio

Keith Hastings
ERC/Jacobs Sverdrup Technology, Huntsville, Alabama

National Aeronautics and
Space Administration

Glenn Research Center
Cleveland, Ohio 44135

April 2006

Level of Review: This material has been technically reviewed by technical management.

Available from

NASA Center for Aerospace Information
7121 Standard Drive
Hanover, MD 21076–1320

National Technical Information Service
5285 Port Royal Road
Springfield, VA 22161

Available electronically at http://gltrs.grc.nasa.gov

Effects of Hydrogen on GRCop-84

David L. Ellis
National Aeronautics and Space Administration
Glenn Research Center
Cleveland, Ohio 44135

Keith Hastings
ERC/Jacobs Sverdrup Technology
Marshall Space Flight Center
Huntsville, Alabama 35812

Abstract

This report is a section of the final report on the GRCop-84 task of the Constellation Program and incorporates the results obtained between October 2000 and September 2005 when the program ended.

GRCop-84 contains approximately 5.5 wt% Nb. Nb can react with H and embrittle easily (refs. 2 through 11). Previous work had indicated the thermodynamic possibility that Cr_2Nb could react with H and form niobium hydrides in the presence of high pressure H such as seen in the Space Shuttle Main Engine (ref. 12). In this study, samples were charged with H and then tested in both high pressure H and He environments to determine if measurable differences existed which indicate that hydrogen embrittlement occurs in GRCop-84. Tensile, notched tensile, stress rupture and low cycle fatigue properties were surveyed. High pressure H environment stress rupture testing resulted in a lower reduction in area than a high pressure He environment, and the LCF lives at high strain ranges fall below the lower 95 percent confidence interval for the baseline data, but in general no significant differences were noted either between H and He environment tests or between hydrogen charged materials and the baseline, uncharged extruded GRCop-84 data sets. There was also no discernable evidence of the formation of hydrides or changes in fracture morphology indicating hydrogen embrittlement occurred.

Introduction

Hydrogen embrittlement was identified in the technical literature as long ago as 1875 (ref. 1) and was likely known on a practical level well before then. It is well known that Nb (refs. 2 through 10) and Nb containing alloys (ref. 11) are susceptible to hydrogen embrittlement. Nb readily forms both hydrides and a solid solution with hydrogen. This raises the concern that in the high pressure hydrogen environment of a regeneratively cooled hydrogen fueled rocket engine GRCop-84 may become hydrogen embrittled. Limited testing was undertaken to determine if significant changes in mechanical properties occur after charging GRCop-84 in a high pressure hydrogen environment.

A prior study (ref. 12) examined the thermodynamics of GRCop-84 in a hydrogen environment. The conclusion was that the susceptibility to hydrogen embrittlement would largely be controlled by the chemistry of the Cr_2Nb precipitates found in GRCop-84, temperature and hydrogen pressure. The Cr-Nb phase diagram (ref. 13) indicates that Cr_2Nb has a range of compositions which implies that it has a range of Nb activities. If GRCop-84 is Nb rich (more Nb than the amount needed to form Cr_2Nb), the activity of the Nb in the Cr_2Nb will be unity, and the alloy will act much like pure Nb. The only difference is that the activity of Nb will decrease as the Nb is consumed forming niobium hydride (NbH_x). This does provide a self-limiting mechanism to minimize hydrogen embrittlement, but the hydride would still present a serious problem given its much greater specific volume.

If GRCop-84 is made Cr rich, the activity of Nb is greatly reduced. Hydride formation in the form of $Nb_{0.59}H_{0.41}$ does remain a possibility in a 35 MPa (5 ksi) hydrogen environment, but the pressure required rises to 462.2 MPa at 100 °C (212 °F). At even moderately higher temperatures such as 150 °C (302 °F),

the hydrogen pressures required to form the hydrides rapidly exceeds 101 GPa (14 Msi). This limits the probability and amount of hydride formation that could occur. In contrast, pure Nb requires only a partial pressure of 1.93×10^{-6} MPa (2.8×10^{-4} psi) to form niobium hydride at 100 °C.

Based on prior work (ref. 12), it was never thermodynamically favorable to form a Nb-H solid solution in the Cr_2Nb or the alloy.

While thermodynamics indicate that GRCop-84 could potentially form hydrides and be embrittled, the kinetics of the process are unknown. It is assumed based on the small size of the absorbed hydrogen atom and the generally high diffusivity of hydrogen in all solids that the process would not be diffusion limited. Unfortunately no data exists on the interaction between hydrogen and Cr_2Nb.

If hydrides do form, they should decrease the ductility and the energy needed to propagate cracks. Tensile and low cycle fatigue testing should show differences between standard air, vacuum or inert atmosphere tests and the corresponding high pressure hydrogen tests. Stress rupture testing can also reveal time dependent phenomena that may be occurring. Evidence of hydrides should also be visible on the fracture surfaces of the failed samples, and a hydrogen solid solution would likely result in a discernable change in dimple size and morphology or even failure mode.

With these potential problems in mind, the specification for GRCop-84 was written to include a slight excess of Cr in the alloy. This minimizes the activity of Nb in the alloy and vastly reduces the potential risk of GRCop-84 undergoing hydrogen embrittlement. This work is meant to confirm that the approach used alleviates these concerns.

Experimental Procedure

Three types of testing were done – tensile, stress rupture, and LCF. Due to the needs of the Columbia Accident Investigation Board and the Return To Flight Program for Marshall Space Flight Center (MSFC) facilities and personnel, not all analysis was as in-depth as originally planned. Mainly this involved limiting post test examination of the specimens to selected specimens rather than all specimens.

Sample Charging

All samples were charged with hydrogen prior to testing. The samples were made from small GRCop-84 extrusions produced using Crucible Research powder during the RLV Focused Program. The samples were machined into the appropriate test specimen prior to charging. No post machining annealing was done to remove residual or surface stresses.

Samples were charged by heating the samples to 649 °C (1200 °F) in 34.5 MPa (5 ksi) hydrogen for 8 hr. After charging the samples were stored in liquid nitrogen until they were ready to test. Testing began immediately after charging and was completed as quickly as possible to minimize loss of hydrogen from the samples.

Tensile Testing

All high pressure He and H tensile testing was conducted at the NASA MSFC Hydrogen Testing Facility. Samples were tested in a 34.5 MPa (5 ksi) gaseous helium (GHe) or gaseous hydrogen (GH) environment. Testing was conducted at ambient temperature and 500 °C (932 °F). Two sample geometries were used. The first was the smooth sample shown in figure 1. The second was the notched sample shown in figure 2 with a stress intensity factor (K_t) equal to 6.3±0.5.

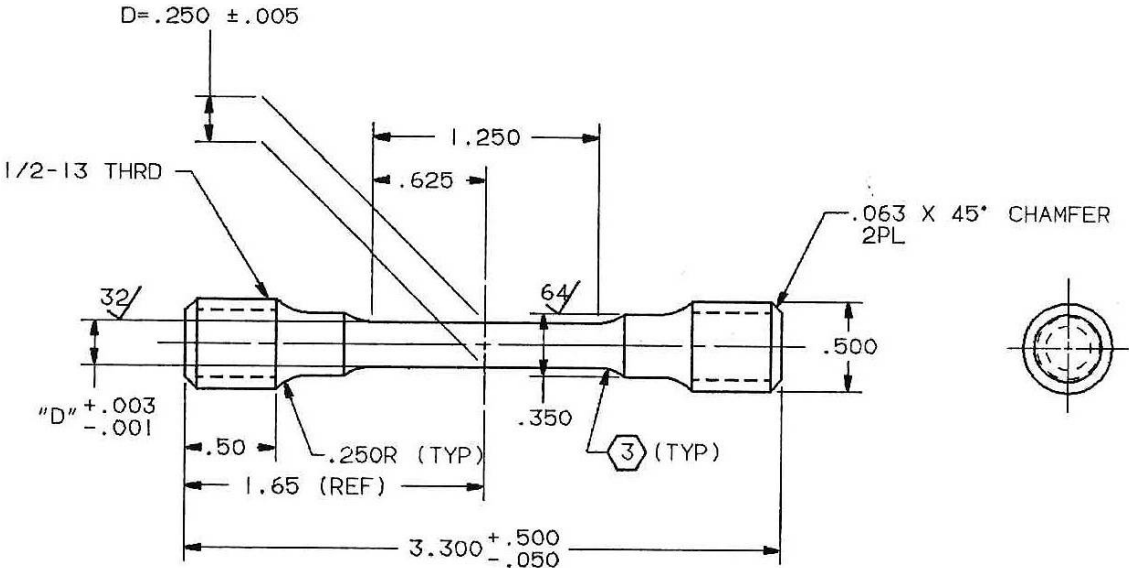

Figure 1.—Smooth tensile specimen.
(Specimen design and drawing courtesy of Pratt & Whitney Rocketdyne)

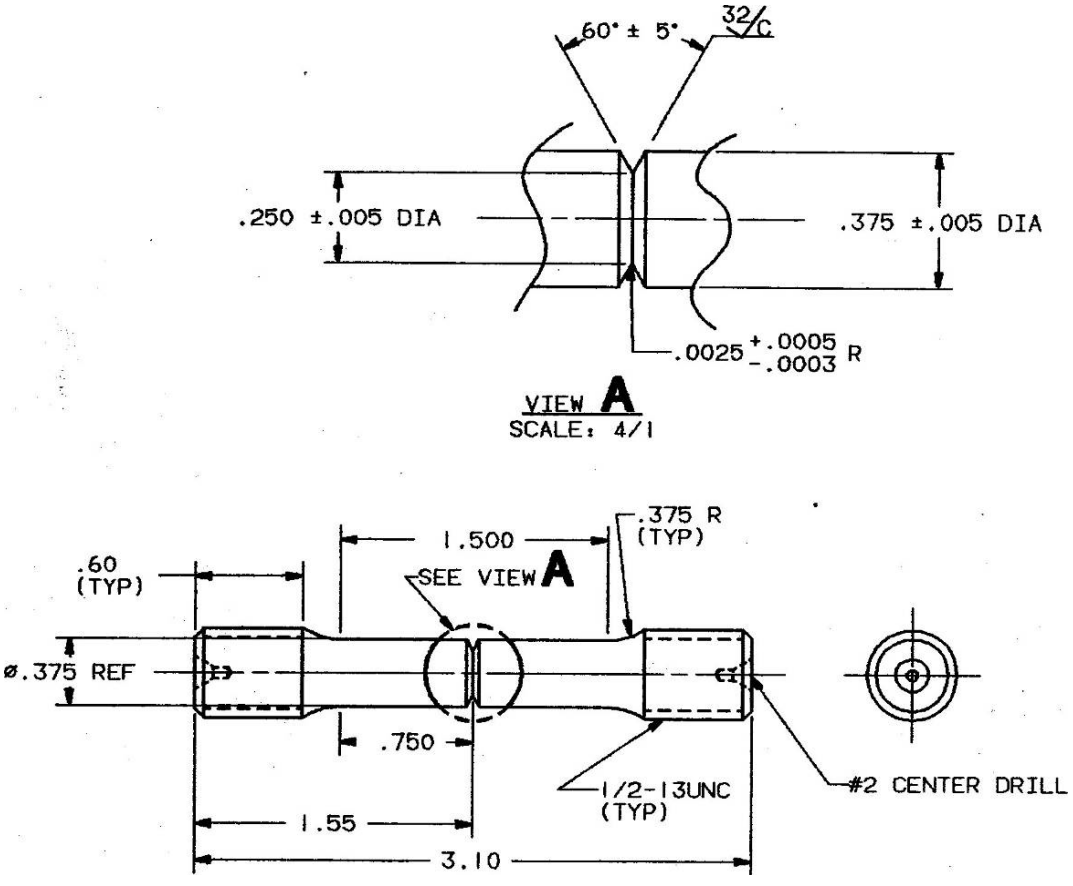

Figure 2.—Notched tensile specimen (K_t = 6.3).
(Specimen design and drawing courtesy of Pratt & Whitney Rocketdyne)

A modified Instron load frame designed to operate in high pressure hydrogen or helium environments was used for testing the samples. Tests were conducted using crosshead control. A crosshead speed of 0.0021 mm/s (0.005 in/min) was selected for these tests. The initial strain rate of these tests corresponds to the initial strain rate for the other tensile tests reported in this task, but the strain rate decreases by up to 25 percent as the sample lengthens.

An extensometer was used to measure the strain of the samples up to 10 percent, the limit of the extensometer. The load and strain were recorded using a data acquisition and control computer. The total sample elongation was measured after the test using witness marks on the sample.

Stress Rupture Testing

Stress rupture testing was conducted at 500 °C (932 °F) using a stress of 109 MPa (15.8 ksi) in 34.5 MPa (5 ksi) gaseous hydrogen and helium. The testing was performed at the NASA MSFC Hydrogen Testing Facility using a modified Instron tensile load frame. The specimen design is shown in figure 3.

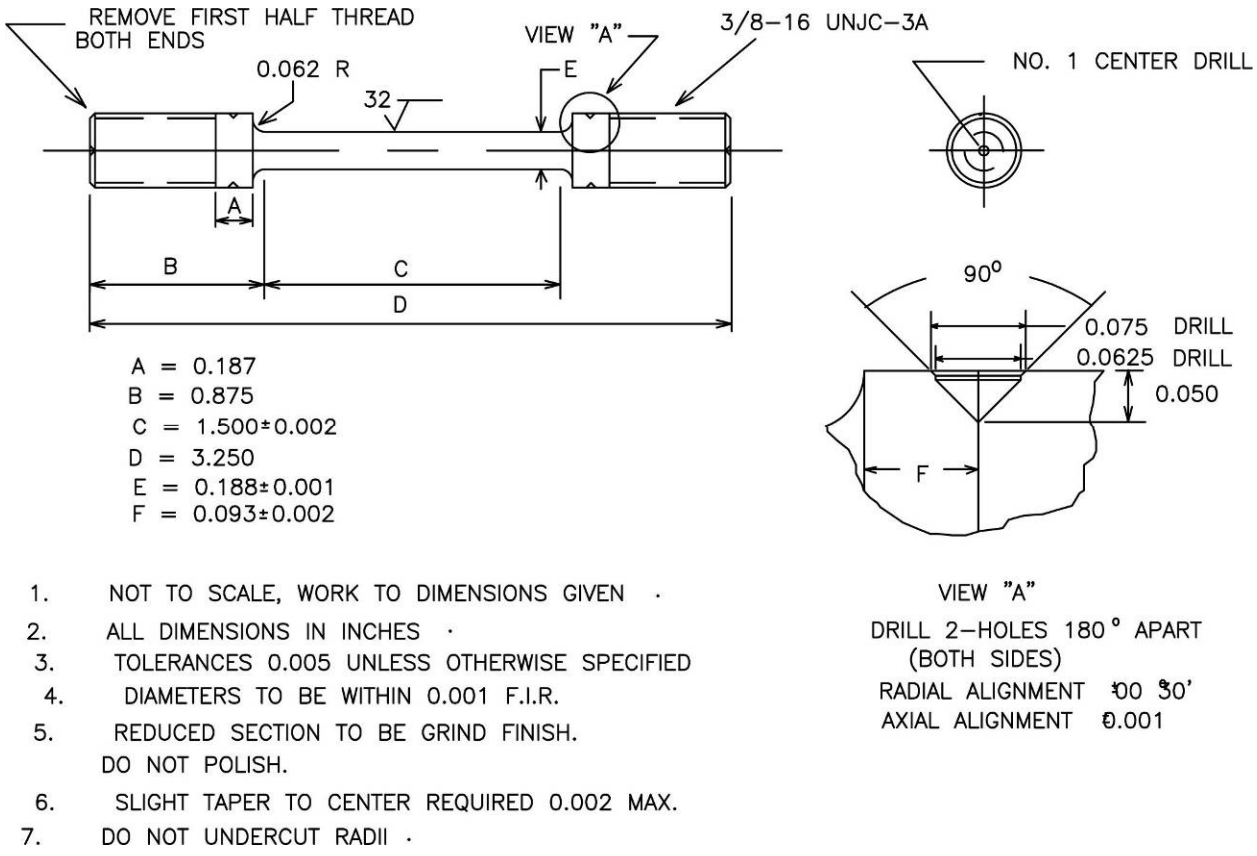

Figure 3.—Stress rupture specimen design.
(Specimen design and drawing courtesy of NASA MSFC)

Low Cycle Fatigue Testing

Low cycle fatigue testing was also conducted at the NASA MSFC Hydrogen Testing Facility. The specimen design used is shown in figure 4. Testing was done in strain control mode. A triangular waveform with a frequency of 10 cycles per minute (0.167 Hz) was used for the tests.

Fractography

Fractography was conducted at NASA Glenn Research Center following completion of the mechanical testing. All samples were first examined with an Olympus SZH optical macroscope with DP12 digital camera to determine the general morphology of the fracture surfaces.

A JEOL 840A Scanning Electron Microscope (SEM) was used for most of the detailed fractography. The SEM door allowed the samples to be inserted without the need to cut the samples. This prevented contamination of the fracture surface during a cutting step.

Six LCF samples were also observed using a Hitachi Field Emission Scanning Electron Microscope (FESEM). The FESEM had significantly greater resolution and could easily operate at magnifications in excess of 100,000×. This was critical in determining if fine bubbles formed during LCF testing. The samples could be inserted on their side and rotated to an upright position in the microscope, so cutting was not required for these samples either.

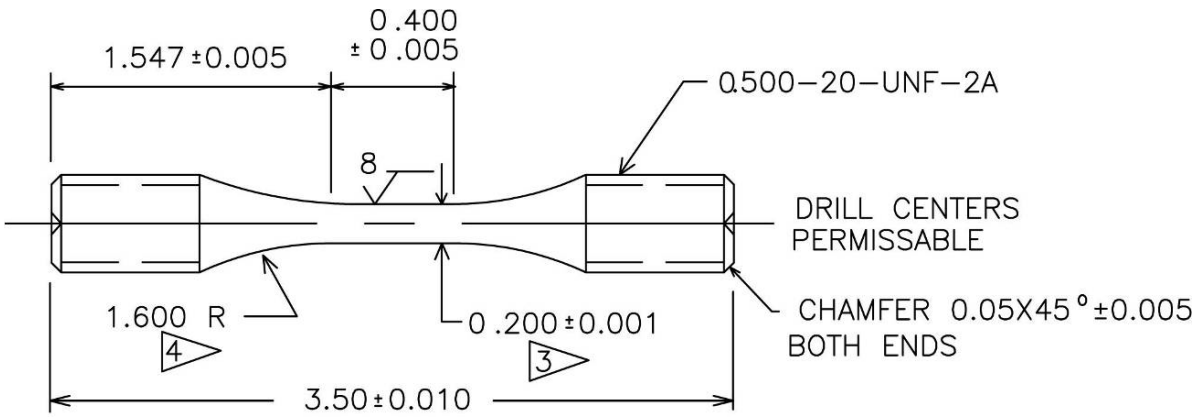

1. NOT TO SCALE, WORK TO DIMENSIONS GIVEN
2. ALL DIMENSIONS IN INCHES
3. SLIGHT TAPER TO CENTER REQUIRED (0.002 MAX)
4. DO NOT UDERCUT RADII
5. NO TRANSVERSE TOOL MARKS IN $\sqrt{8}$ FINISHED AREA
   POLISH ALONG AXIS
6. ALL DIAMETERS CONCENTRIC WITHIN 0.005 TIR
7. UNSPECIFIED TOLERANCES ±0.005 INCHES

Figure 4.—Low cycle fatigue (LCF) specimen.
(Specimen design and drawing courtesy of NASA MSFC)

Results

Tensile Testing

Typical stress-strain curves for GRCop-84 samples are shown in figure 5. For comparison, a typical room temperature stress-strain curve for GRCop-84 samples is shown as well. No 500 °C (932 °F) testing was conducted on the baseline material, so no corresponding stress-strain curve is presented. However, based upon the 400 and 600 °C (752 and 1112 °F) tensile curves for the baseline material, it is expected that the 500 °C stress-strain cure for the baseline GRCop-84 would be very similar to the GH and GHe 500 °C curves.

Figure 6 shows the average tensile strength of the samples tested in GHe and GH. For the notched tensile samples, the specimens all failed in the notch before the smooth section attained 0.2 percent strain. There is therefore no measured 0.2 percent yield strength. The bars represent the average of three tests, and the lines represent one standard deviation above and below the average.

Figure 7 shows the elongation of the specimens. The notched samples are not shown because the samples failed in the notch before significant deformation (>0.5 percent) was measured. The bars again represent the average of three tests, and the lines represent one standard deviation above and below the average.

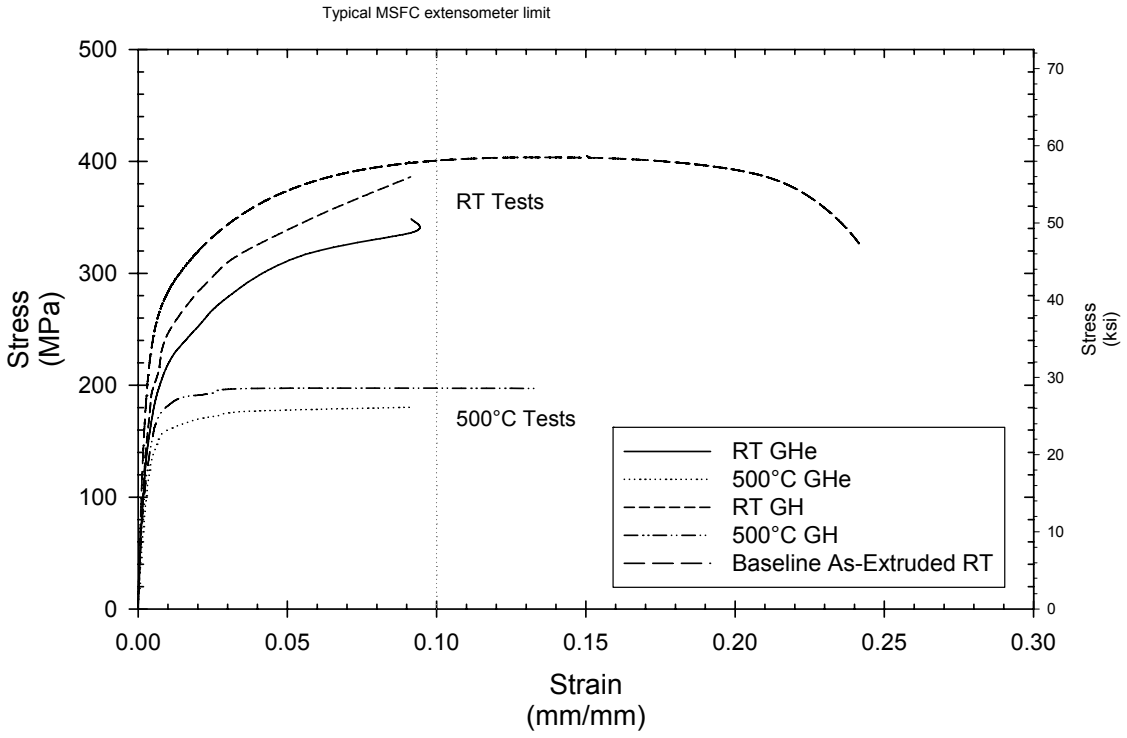

Figure 5.—Typical GRCop-84 stress-strain curves.

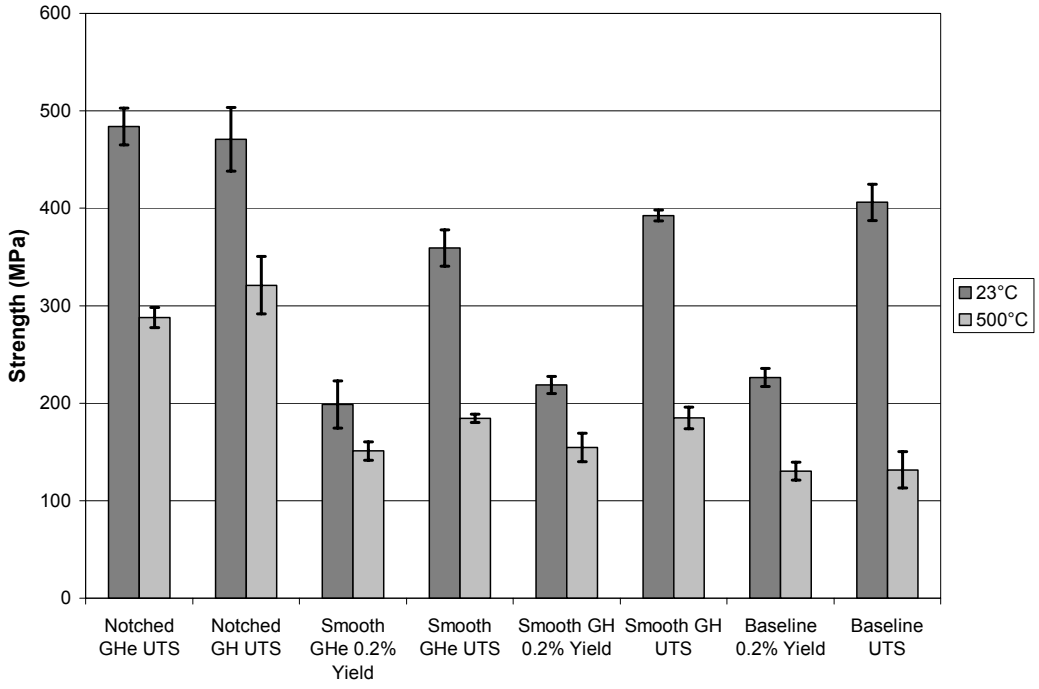

Figure 6.—Average tensile strength of GRCop-84 tested in high pressure gaseous He and H.

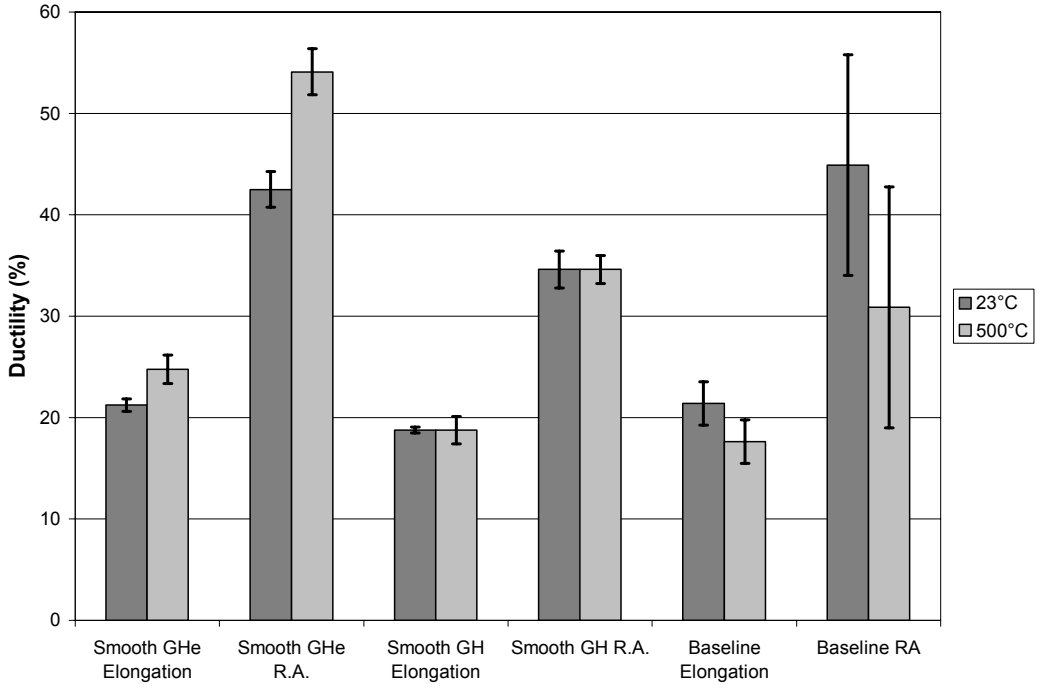

Figure 7.—Average tensile ductility of GRCop-84 tested in high pressure gaseous He and H.

For comparison purposes the baseline tensile properties of GRCop-84 are also presented. The values for room temperature tests represent the average of five tests, and the lines again represent one standard deviation above and below the average. While no data was available for the baseline alloy tested at 500 °C, the tensile properties of the baseline data were calculated from the regression models for GRCop-84 (ref. 14). These models include the ability to determine the standard deviation at each temperature, and those values are included in the bar graphs as well.

Statistical analysis was conducted on the tensile data. At a 95 percent confidence level there was no statistically significant difference in the average yield strengths for the smooth tensile specimens and the baseline tests. For the ultimate tensile strength, the notched specimens had a statistically greater strength than the smooth tensile specimens and the baseline specimens at 500 °C. At room temperature the notched specimens had statistically equivalent ultimate strengths at a 95 percent confidence level. The ultimate tensile strengths for the smooth tensile specimens and the baseline specimens were statistically equivalent at a 95 percent confidence level.

The elongation and reduction in areas for the smooth tensile specimens tested in gaseous hydrogen and helium and the baseline specimens are statistically equivalent at a 95 percent confidence level. This result may be partially influenced by the high variability in the baseline specimens' reduction in area and should be used with some caution.

Figure 8 shows the fracture surface of representative notched and smooth tensile specimens. For comparison a typical fracture surface for GRCop-84 without hydrogen charging tested in air at room temperature is included. All samples show evidence of ductile failure. No major change in fracture mechanism from the normal microvoid coalescence was observed. The notched samples had some evidence of more angular failure surfaces, but the differences were minimal and are a subjective opinion based upon observations of only a few samples. As shown in figure 9, even at the root of the notch GRCop-84 specimens showed ductile rather than brittle fracture, and the failure mode was consistent with all other tensile test specimens.

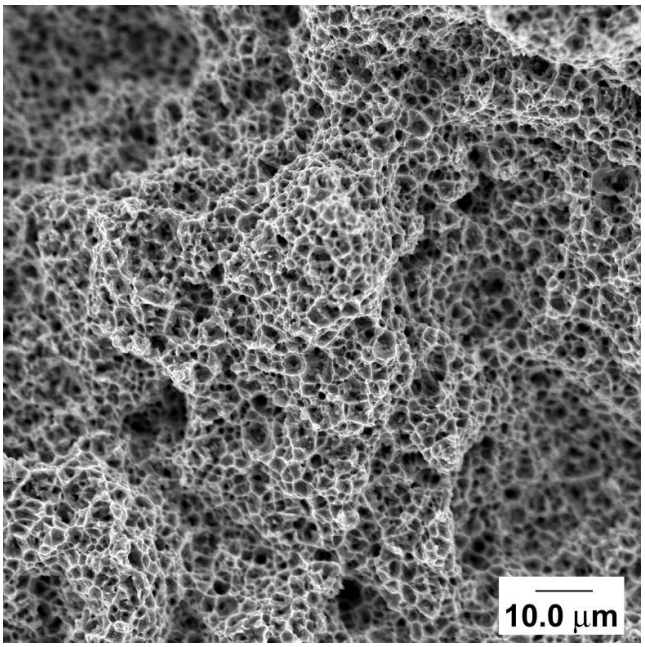

(a) Baseline, uncharged GRCop-84 specimen tested in air at room temperature.

Figure 8.—Fracture surfaces of GRCop-84 tested in high pressure hydrogen and helium.

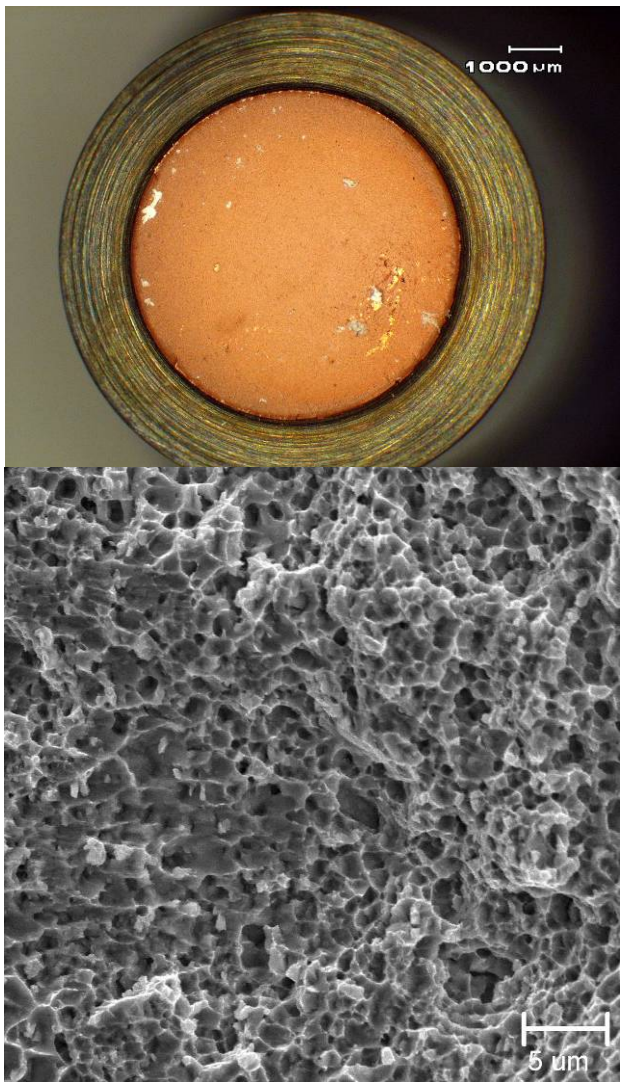

(b) Notched specimen tested in GH at room temperature

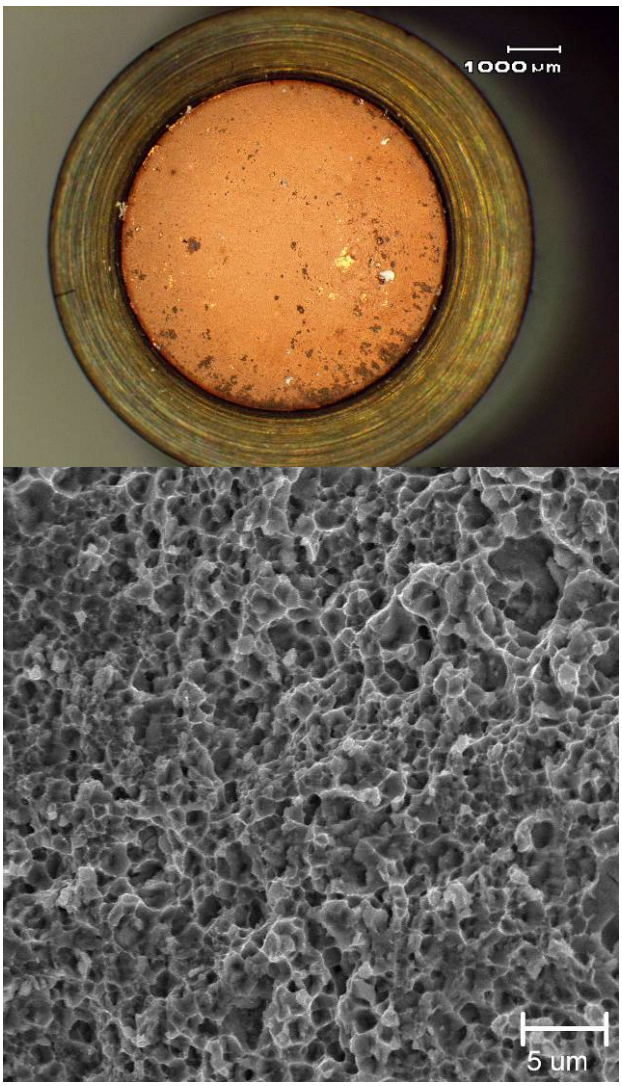

(c) Notched specimen tested in GHe at room temperature

Figure 8.—Continued.

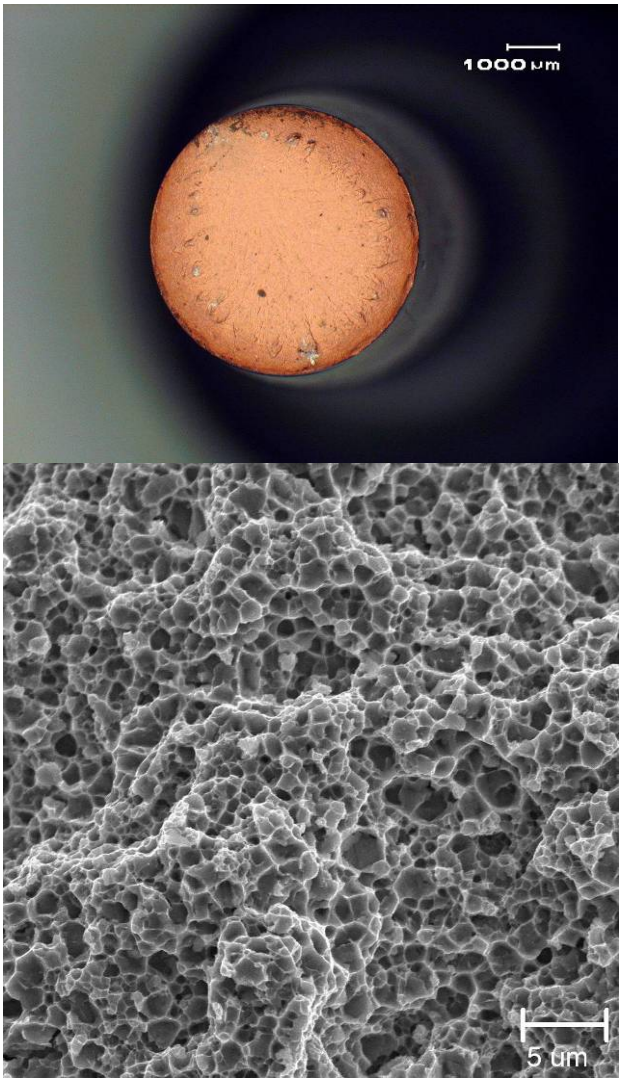

(d) Smooth specimen tested in GH at room temperature

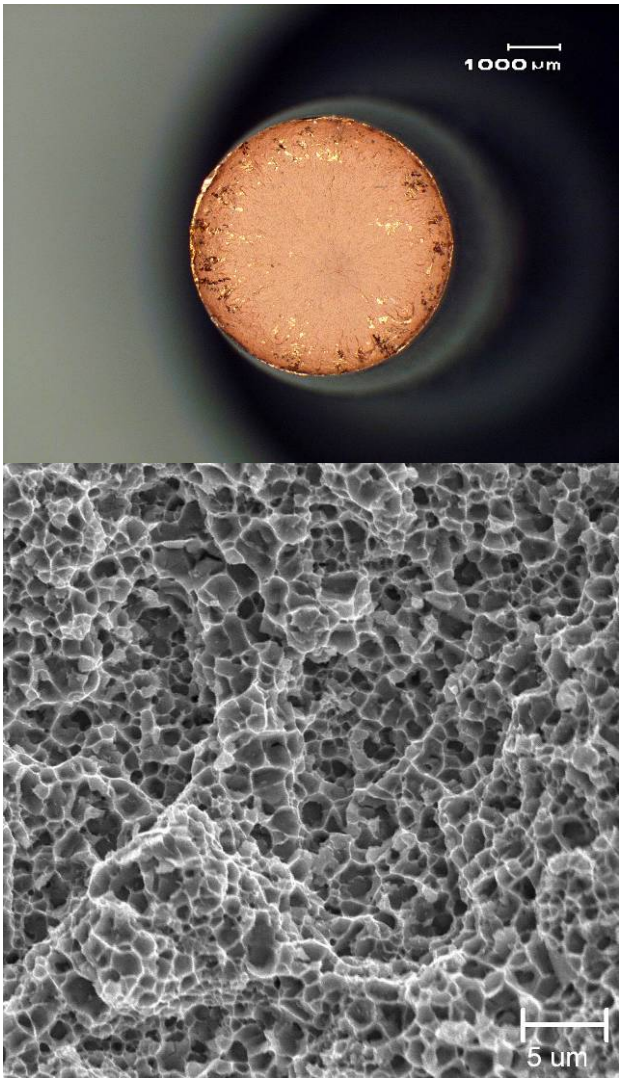

(e) Smooth specimen tested in GHe at room temperature

Figure 8.—Continued.

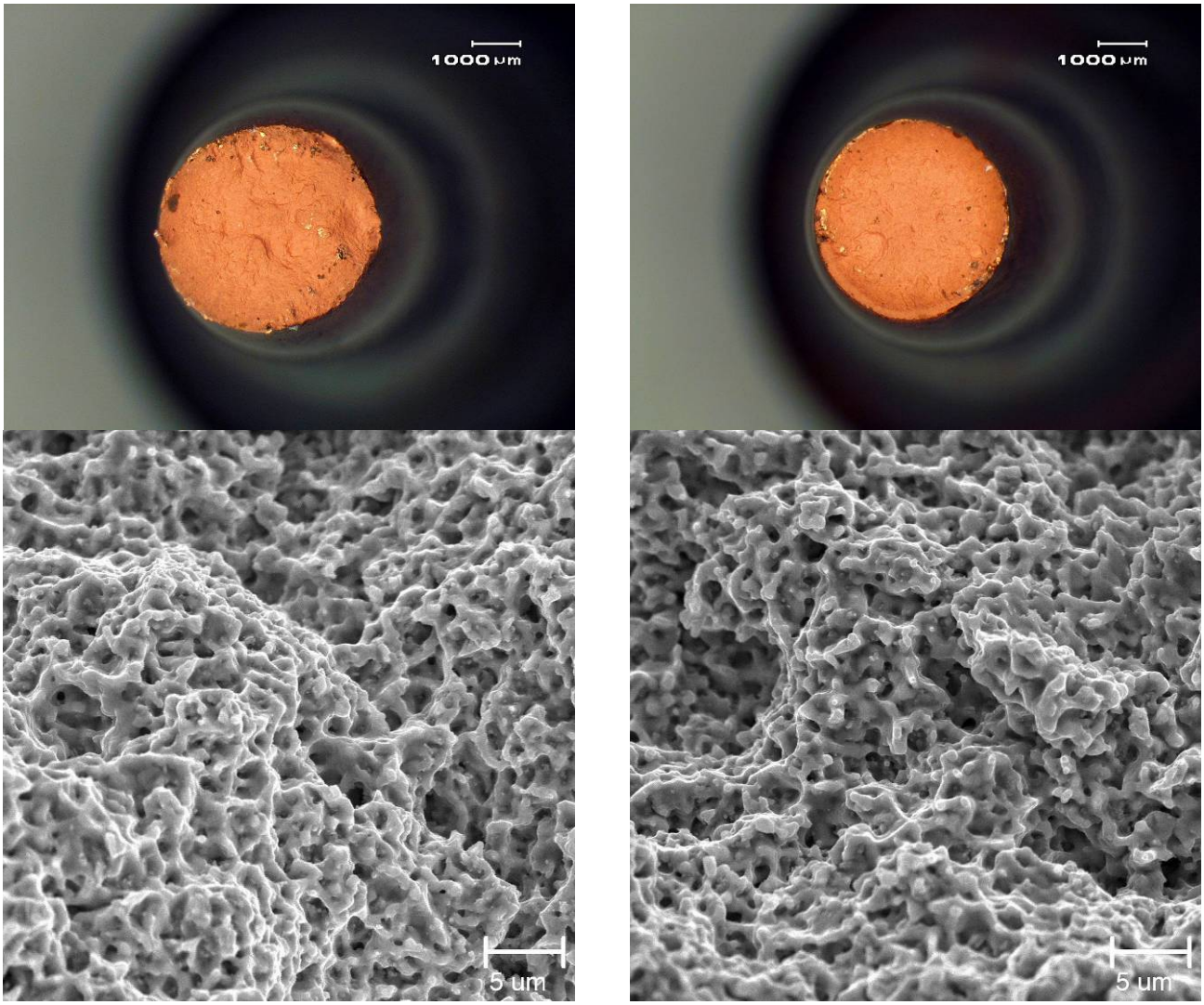

(f) Smooth specimen tested in GH at 500 °C (932 °F) (g) Smooth specimen tested in GHe at 500 °C (932 °F)

Figure 8.—Concluded.

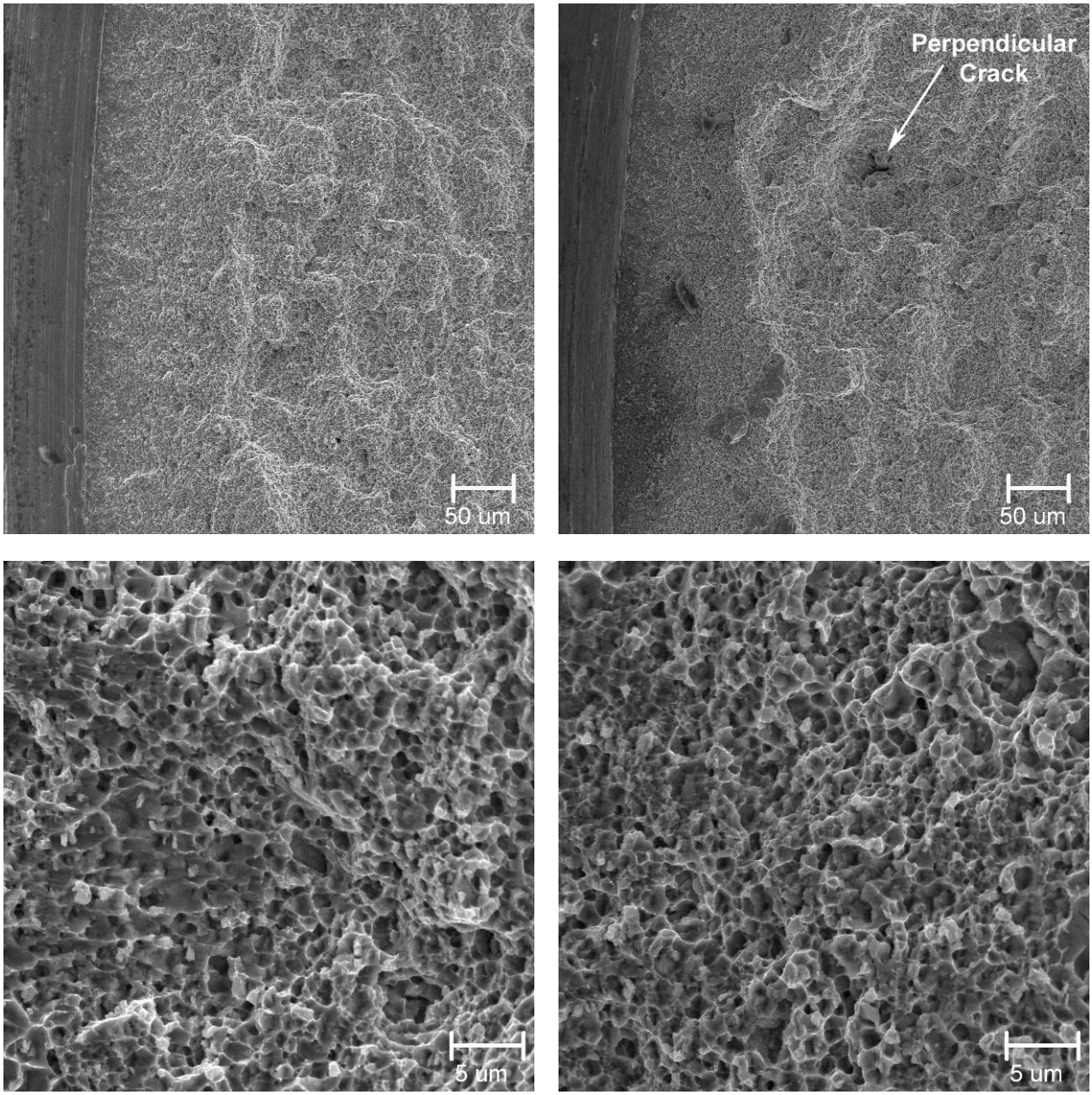

(a) Notched specimen tested in GH at room temperature

(b) Notched specimen tested in GHe at room temperature

Figure 9.—Fracture surfaces at the notch root of GRCop-84 notched tensile specimen tested at room temperature.

Stress Rupture

Table 1 summarizes the measured reductions in areas for the specimens and the stress rupture lives. The identification of two samples was lost, so the reduction in area for those samples could not be reported. For comparison, the average values for the uncharged samples creep tested at NASA GRC under the same conditions are also included. For the vacuum creep testing, the reduction in area did not vary greatly with temperature and stress. The average for all specimens was a 16.2 percent reduction in area.

TABLE 1.—REDUCTION IN AREA FOR HYDROGEN CHARGED GRCop-84 STRESS RUPTURE SPECIMENS

Test environment	Sample	Reduction in area (%)	Stress rupture Life (h)
GH	1		35.6
	2		61.5
	3	7.9	22.2
	Average	7.9	39.8
GHe	4	60.2	50.5
	5	66.8	99.4
	Average	63.5	75.0
Vacuum (Uncharged specimens)	Average	13.1	20.1

The displacement of the samples during the testing was recorded using a strip chart. The resolution of the chart was insufficient to determine the creep rates of the samples, so only the lives are presented.

Two unexpected results from the stress rupture testing were the increase in life and reduction in area for the samples tested in GHe. While the increase in life is not statistically significant, the difference in average life is sufficiently large that is suspected that larger data sets with six or seven tests in each environment would yield a statistically significant difference. The difference in the reduction in areas cannot be statistically analyzed, but the nearly tenfold increase for the GHE tests strongly suggests a major change in the reduction in area between the two environments.

Figure 10 shows the fracture surfaces of the stress rupture specimens. The failures are consistent with respect to each other and prior creep specimens tested in vacuum at NASA GRC. The failure mode appears to remain microvoid coalescence and growth as is observed with the tensile specimens (figs. 8 and 9). Arguably the fracture surfaces exhibit some more angularity than those for the prior creep testing, but there again there was no gross change in fracture mode.

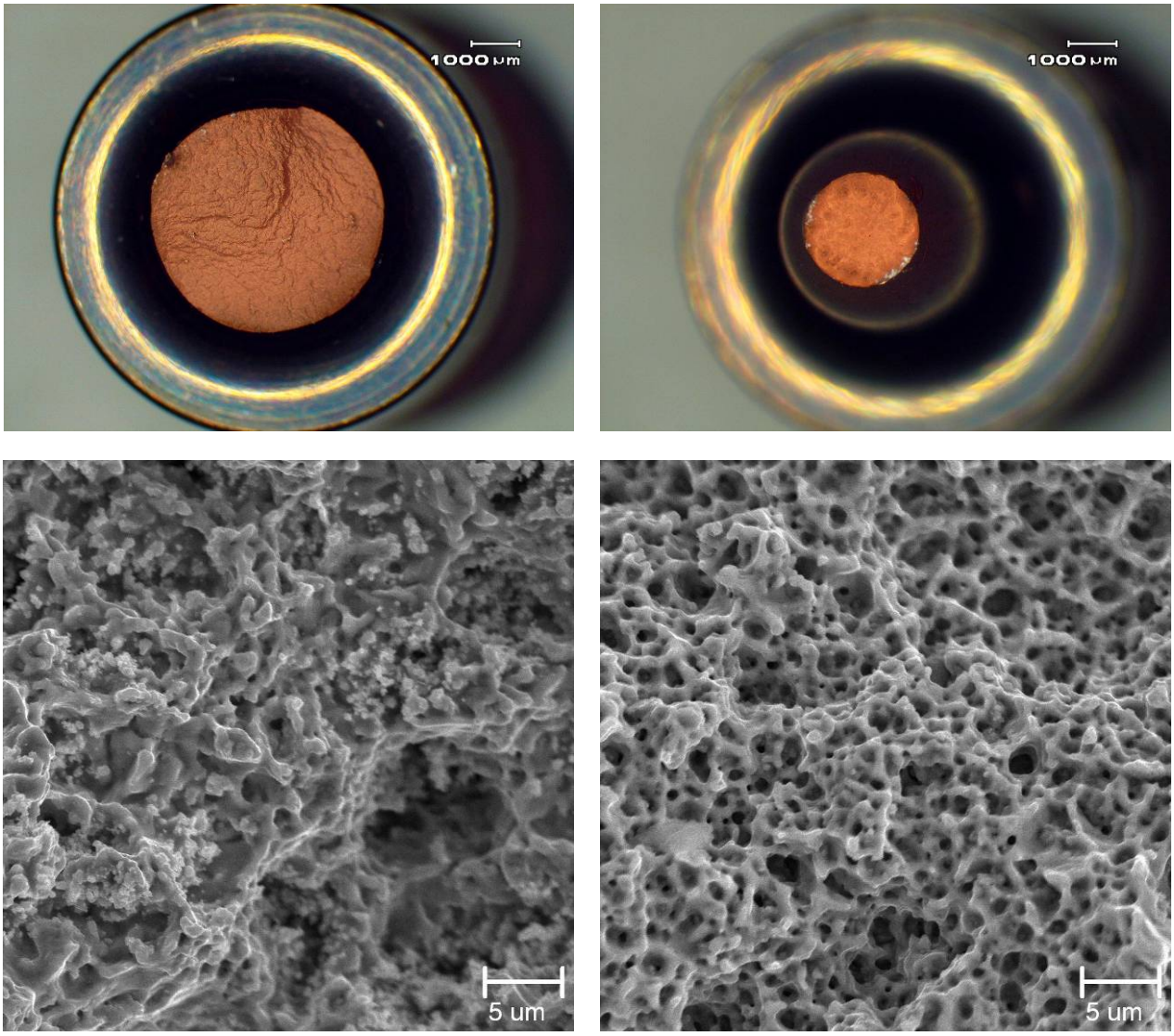

(a) Creep tested at 500 °C (932 °F)/109 MPa in 34.5 MPa (5 ksi) GH

(b) Creep tested at 500 °C (932 °F)/109 MPa in 34.5 MPa (5 ksi) G He

Figure 10.—Fracture surfaces of GRCop-84 stress rupture specimens.

Low Cycle Fatigue

The LCF tests were run in strain control. Table 2 gives the average minimum and maximum resultant stresses experienced by the samples at the three strain levels tested. The average stresses for GH and GHe were statistically equivalent at each total strain level, so the data was pooled for a single average at each test condition.

TABLE 2.—AVERAGE RESULTANT STRESSES DURING LCF TESTING

Total strain range (%)	Minimum resultant stress	Maximum resultant stress
0.7	–266.6 MPa (–38.64 ksi)	173.1 MPa (25.08 ksi)
1.2	–317.5 MPa (–46.02 ksi)	213.4 MPa (30.93 ksi)
2.0	–370.5 MPa (–53.69 ksi)	247.8 MPa (35.91 ksi)

The life results for the room temperature LCF tests appear in figure 11. The data for the GH and GHe tests were compared at each strain range. As with the resultant stresses, it was determined at each total determined at each total strain range that there was no statistically significant difference in the average of the common logarithm of the lives of each test. As a result the data for the GH and GHe tests could be pooled. A regression was then performed on the pooled data to generate the linear regression line in figure 11. For comparison the average baseline room temperature LCF lives of GRCop-84 tested in argon and the one-sided lower 95 percent confidence interval are also presented.

The general morphologies of the LCF failures were also examined. An example of one of the fracture surfaces that demonstrates the initiation and growth of the LCF cracks is shown in figure 12. The initiation site remains at or very near the surface which is consistent with other LCF testing (ref. 15). The cracks propagate through the sample until tensile overload occurs and the sample breaks. Fractography was conducted on the LCF specimens to determine if grain boundary decohesion occurred or if hydrogen bubbles formed during testing. The results of the fractography are shown in figure 13. An FESEM was used to maximize the resolution and magnification to look for the small features expected. Some debris and surface oxidation that occurred after the testing was noted, but there was no evidence of grain boundary decohesion or hydrogen bubble formation even at very high magnifications (fig. 14).

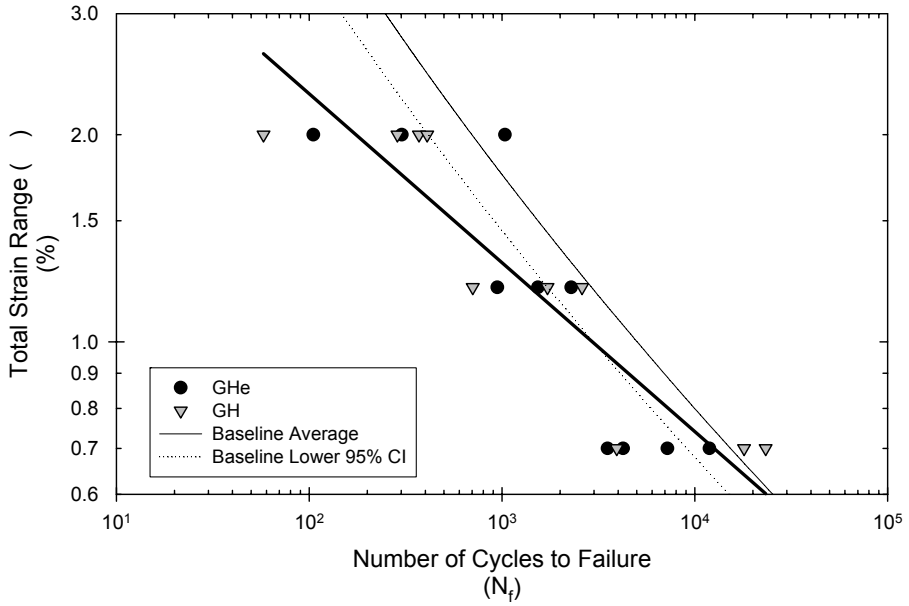

Figure 11.—Low cycle fatigue lives of GRCop-84 tested in high pressure gaseous He and H.

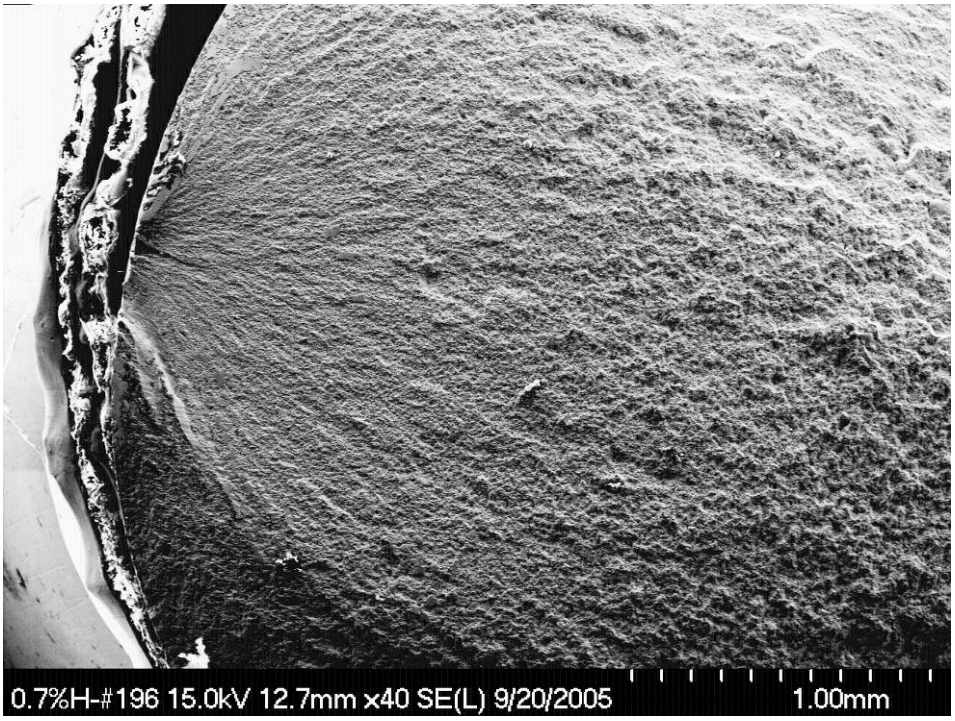

Figure 12.—Representative LCF fracture surface of hydrogen charged GRCop-84. (0.7% $\Delta\varepsilon_{Total}$ specimen tested in GH)

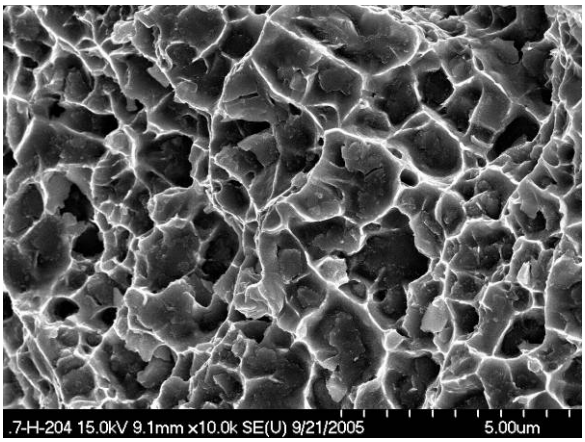

(a) 0.7% $\Delta\varepsilon_{Total}$, GH

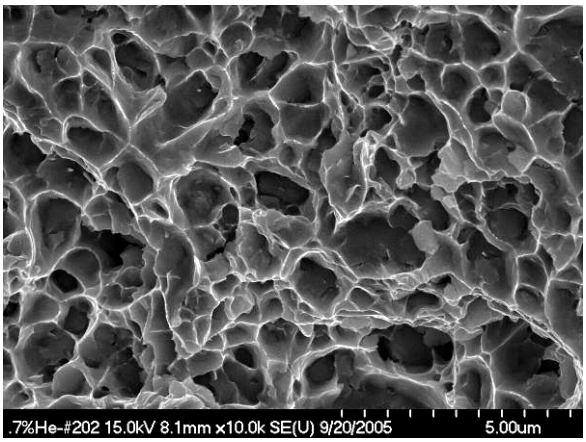

(b) 0.7% $\Delta\varepsilon_{Total}$, GHe

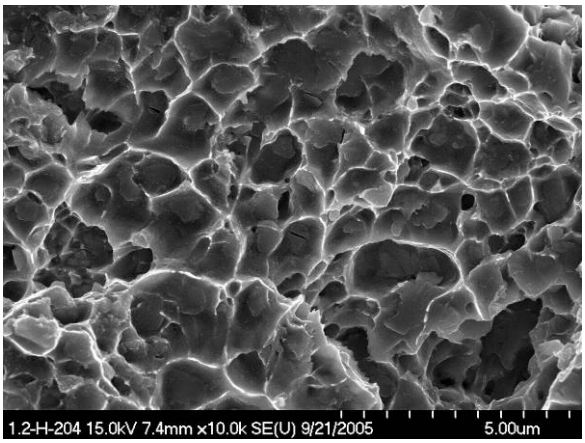

(c) 1.2% $\Delta\varepsilon_{Total}$, GH

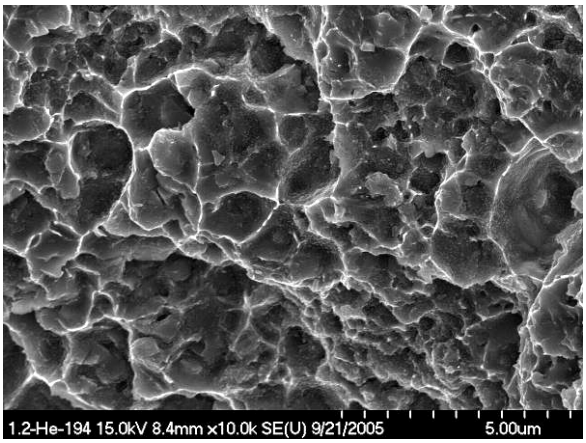

(d) 1.2% $\Delta\varepsilon_{Total}$, GHe

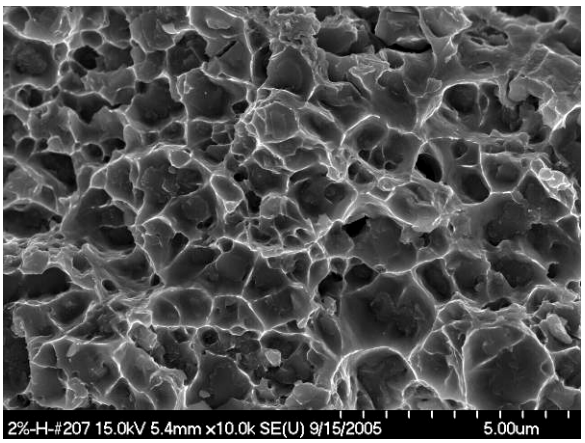

(e) 2.0% $\Delta\varepsilon_{Total}$, GH

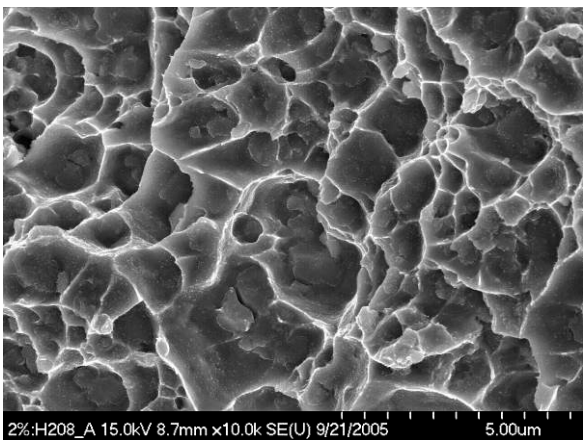

(f) 2.0% $\Delta\varepsilon_{Total}$, GHe

Figure 13.—Fracture surfaces of hydrogen charged GRCop-84 LCF specimens testing in GH and GHe.

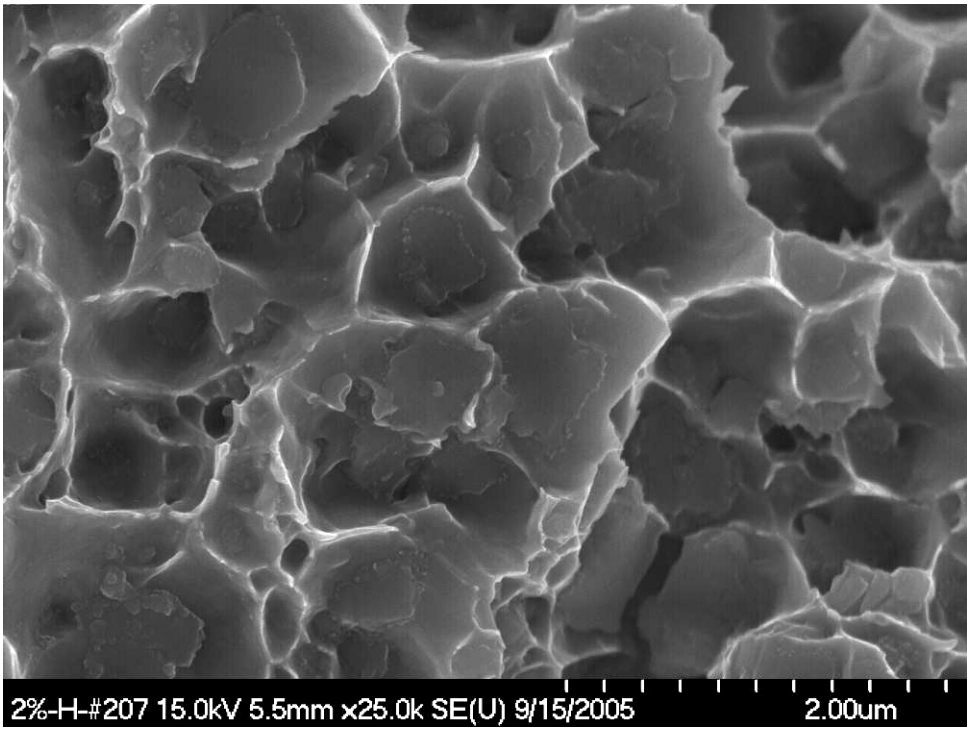

Figure 14.—High magnification image of LCF surface showing lack of grain boundary decohesion and hydrogen bubble formation in 2.0 percent $\Delta\varepsilon_{Total}$, GH sample.

Discussion

Tensile Testing

By soaking GRCop-84 in high pressure hydrogen for an extended period of time at an elevated temperature, the samples were subjected to conditions that mimic the operation of a main combustion chamber liner and promote Internal Hydrogen Embrittlement (IHE). This exposure will help determine if hydrides can form in the alloy and if they have any measurable effect. For this set of samples the ductility remains good, and the strengths of the specimens are equivalent to uncharged specimens. No changes in the fracture surfaces were observed. Therefore it was concluded that no evidence of hydride formation was observed.

This result is consistent with the results of Spitzig et al. (ref. 1) for a Cu-20 vol% Nb composite. Their earlier work had indicated that H would embrittle Nb at room temperature if the H concentration exceeded 1.5 at.% (ref. 2). After charging the composite to a concentration of 1.95±0.07 at.% H the composite still exhibited a ductile failure with little or no change in ductility. Spitzig at al hypothesized that a favorable hydrostatic stress state on the Nb filaments was established in the Cu-20 vol% Nb composite by the Cu matrix. This prevented a change in the fracture mechanism and allowed the composites to remain ductile. If this is the case, the same mechanism is likely present in the GRCop-84 specimens and would contribute to the alloy remaining ductile even after hydrogen charging.

The effect of hydrogen on the Cr_2Nb phase and GRCop-84 may also be mitigated by the high hardness and low ductility of this Laves phase. Unlike pure Nb where the ductility of the metal is above 30 percent (ref. 3) and can decrease substantially, Cr_2Nb is inherently very brittle (refs. 4 and 5). As a result of the lower ductility, any effect of hydrogen on Cr_2Nb may not be readily observable especially in a macroscopic test such as a tensile test.

Testing in hydrogen allows for the observation of Hydrogen Environment Embrittlement (HEE). HEE is a surface phenomena related to the exposure of new surfaces to hydrogen and their embrittlement. If a

crack forms and propagates, HEE can help propagate the crack much faster than in air or an inert atmosphere such as the high pressure He. Preexisting notches and cracks are prime locations for hydrogen to gather and embrittle a material.

Examining the notched specimens, both sets (GHe and GH) failed in the notch. Deformation outside the notch was minimal. Given the design with the notch in the center, this is expected. The lack of premature failure, no change in the fracture mode from ductile to brittle and a strength ratio of the samples tested in GH to samples tested in GHe near 1 indicate that the hydrogen charged samples did not develop notch sensitivity at $K_t = 6.3$ for the high pressure hydrogen environment. The higher UTS values for the notched samples relative to the smooth samples are likely a reflection of the concentration of the deformation and stresses into a much smaller volume that approaches a plane strain or even a uniaxial stress condition. The physical constraints and stress states when shear stresses are minimized or eliminated will increase the observed ultimate tensile strength. In addition, the hydrostatic pressure exerted by the 34.5 MPa (5 ksi) gas environment will tend to promote more ductility, extra uniform elongation and higher strength. Given this combination of constraints and hydrostatic compressive stress it is not surprising that the strength results for the notched specimens are better than those for smooth GRCop-84 samples tested at atmospheric pressure.

A small number of cracks roughly perpendicular to the fracture surface such as one seen in figure 9(b) were observed on the fracture surfaces of the notched tensile specimens. Past experience has shown that the cracks are normally associated with large Cr_2Nb particles which were not dissolved during the melting process. Careful examination of the cracks revealed that several had 2 to 10 μm Cr_2Nb particles associated with the cracks. The observable failed Cr_2Nb particle-copper matrix interfaces were still exhibiting a ductile microvoid coalescence type of failure. No evidence of hydrogen bubbles or hydrides was discernable. The fracture of the samples may have been partially aided by these large particles since the failure mode appears to favor fracture at or near these particles, but there was no gross change in the fracture mode observed in these tests.

The overall ductility of the notched specimens was essentially zero. Given the strong localization of the stresses and deformation in and near the plane of the notch, this is not unexpected. In retrospect, for measuring the effect of hydrogen on the ductility and notch sensitivity of GRCop-84, a combination smooth and notched tensile specimen design with the same cross-sectional area in the reduced section and at the bottom of the notch would have been more revealing.

Statistical analysis indicates that there are few differences among the specimens tested. The only difference that occurred was caused by sample geometry, not hydrogen. Based on this set of results, high pressure hydrogen appears to have minimal effects on tensile properties. As a caveat, GRCop-84 should be tested in high pressure He and H after being charged in high pressure He to isolate any potential effects of IHE and thermal exposure as well. It is unlikely that IHE will occur given the equivalency of the baseline and hydrogen charged data, but the high value of the rocket engine and missions make a confirmation prudent. Such work will also increase the meager hydrogen testing data available for GRCop-84.

Stress Rupture

The limited testing of GRCop-84 in GH and GHe showed that specimens tested in GH have lives and reduction in areas equivalent to specimens tested in vacuum. The specimens tested in GHe show longer lives than the specimens tested in GH and most specimens tested in vacuum. Based on prior experience, the creep life can be well estimated by dividing the creep ductility by the steady-state or minimum creep rate since most of the creep occurs in a steady-state or near steady-state condition. While the steady-state creep rate was not be measured, it is likely similar for all three conditions. The increase in lives for GHe specimens appears to come from an increase in ductility.

It was observed that the reductions in area for the specimens tested in GHe were much greater than those for specimens tested in GH or vacuum. The results are somewhat confounded by the failure of the specimens near the transition radius from the gauge to the threaded section, but it appears highly likely

that there is a real change in the reduction in area based upon this small data set. This is one of the few differences noted in the behavior of GRCop-84 in high pressure H and He environments.

Even with the differences in reduction in area the fracture surfaces seen in figure 11 do not indicate a change in failure mode. It appears that the effect of the hydrogen started after the microvoids formed. One possibility is that the hydrogen migrated to the voids and altered the stress state during the test by introducing an internal pressure not found in the helium tests. This would also tend to counteract the hydrostatic pressure of the environment that promotes higher ductility. This study did not test this hypothesis, but it would be possible to fracture the sample and examine the voids that are within the stress rupture specimens using techniques such as Auger microscopy or mass spectrometry to see if hydrogen is present in the voids. In addition, the reduction in areas of the specimens tested in GH, while much lower than those tested in GHe, are similar to the reduction in areas of samples tested in vacuum. This could be indicative of a stress state more similar to the vacuum test, specifically one where the effects of the hydrostatic pressure has been reduced.

HEE may also be a possibility, but the fracture surfaces do not show any evidence of a change in failure mechanism or multiple fracture mechanisms occurring. Expanding the number of stress rupture tests and selecting a different design with a more gradual transition from the grip section to the reduced gauge section would allow for confirmation of this change in behavior. Techniques exist such as mass spectroscopy to determine if there is hydrogen in the subsurface voids. Those were not done during this task, but could yield significant results.

Low Cycle Fatigue

The low cycle fatigue results indicate that there is no statistically significant differences between GRCop-84 tested in high pressure He and H. This indicates that Hydrogen Environment Embrittlement (HEE) is unlikely to be a contributing factor to the growth of fatigue cracks in GRCop-84. This is a significant result since the exposure of fresh Cr_2Nb surfaces to hydrogen could have promoted hydride formation and the build-up of a large volume phase in the crack. This would be analogous to oxidation assisted fatigue crack growth in other alloys. Oxidation-fatigue interactions tend to lower the LCF lives of metals, often significantly (ref. 21). The similarity of the two data sets leads to the conclusion that this is not a significant factor.

The observation was made that as the total strain range increased the lives of GH and GHe specimens deviated negatively from the baseline lives measured for specimens tested in argon. This trend could have resulted from the scatter in the highest strain range data. The two lowest lives at the 2.0 percent total strain range have a strong effect on the regression line shown in figure 11. However, since some hydrogen embrittlement mechanisms can be stress or strain dependent, the specimens were examined further with particular emphasis on comparing low and high strain range specimens.

Internal Hydrogen Embrittlement (IHE) can potentially lower the LCF lives of alloys. The stresses at the crack tip in LCF testing could serve to precipitate niobium hydrides in a manner analogous to titanium (ref. 22) There are considerable differences in the resultant stresses for the three different total strain levels as shown in table 2 with the highest stresses and largest stress range being observed for 2 percent total strain tests. Examinations of the fracture surface even at very high magnifications (fig. 15) did not reveal any changes in the mechanism from a ductile microvoid coalescence mode to a brittle cleavage mode. There was also no evidence of the formation of H bubbles at grain boundaries promoting premature failure or grain boundary decohesion. From this it can be concluded that stress induced precipitation of hydrides does not occur.

The internal stresses generated by the dissolved hydrogen alone could be responsible for a reduction in LCF lives (ref. 23). The LCF life versus strain data does suggest the possibility of hydrogen-dislocation interactions. The dislocation density will increase as the strain range increases especially in the initial stages before the development of persistent slip bands (PSBs). Hydrogen atoms can act to pin the dislocations on an atomic level and generate locally higher stresses and dislocation densities. This would tend to promote crack initiation and growth in fewer cycles and overall lower lives. This hypothesis may

be confirmable using Transmission Electron Microscopy (TEM) of the samples, but no such examination could be done prior to the ending of the task. Alternatively, uncharged specimens can be tested in GHe.

Finally the specimen designs may have played a role in the observed differences in LCF lives. As shown in figure 3, the GH and GHe LCF specimen design uses threaded ends. The baseline data uses a specimen with a smooth end that is gripped in rigid collets during testing. The collet grip has been selected by NASA GRC because it is less likely to become misaligned and promote buckling or shear loads. While no buckling or evidence of shear was observed for the GH and GHe specimens, the possibility of a non-unidirectional stress state cannot be ruled out. Based on historical experience, the problem grows as the strain range increases. This is consistent with the observed deviation in LCF lives.

While a full explanation of the deviation from the baseline data has not been determined, the possibilities of hydride formation, grain boundary decohesion and hydrogen bubble formation have been eliminated. By testing uncharged specimens in GHe the effect of specimen design on LCF life can be assessed. Detailed TEM examination of the dislocations and further testing of uncharged LCF specimens could reveal if the dissolved hydrogen interacts with dislocations and influences the LCF lives.

Future Work

Five items were identified for future work.

1. Baseline GRCop-84 smooth-notched samples with no charging or thermal exposure need to be tested to determine of a notch with stress intensity factor (K_t) of 6.3 is sufficient to cause failure in the notch without any macroscopic ductility in the smooth section. If the samples do exhibit good ductility, the same specimen design should be exposed to 649 °C (1200 °F) for 8 hr to determine if the thermal exposure promotes notch sensitivity.
2. Additional testing and analysis of combined smooth-notched samples should be conducted to further clarify if GRCop-84 suffers a decrease in ductility or notch sensitivity. Samples of the same design should be charged in high pressure He and tested in both high pressure He and H to determine if IHE plays any role in the loss of ductility and apparent notch sensitivity.
3. Stress rupture specimens should be examined to determine if hydrogen has migrated to the microvoids and introduced a pressure within them that lowers the ductility as measured by the reduction in area compared to specimens tested in GHe. Additional samples should also be stress rupture or creep tested at different stresses and temperatures to determine if temperature, stress and time (creep life) play a role in the reduction in ductility.
4. Additional LCF testing should be done on uncharged specimens in GHe to isolate any specimen design effects on the LCF lives as a function of strain.
5. TEM examination of the LCF specimens should be conducted to determine if there are interactions between the hydrogen from the charging of the samples and dislocations during LCF.

Summary and Conclusions

GRCop-84 was tensile, stress rupture and LCF tested in high pressure He and H following charging in high pressure H at 649 °C (1200 °F) for 8 hr.

The tensile results show no statistical difference between the charged samples tested in He or H. Both are also consistent with prior baseline tensile results at room temperature and 500 °C (932 °F). Qualitatively the fracture surfaces showed a consistent failure mode, microvoid coalescence and growth. Notched samples did not exhibit any discernable notch sensitivity, and the fracture mode remained consistent even at the root of the notch. There were small, subtle differences between the fracture surfaces for the notched and smooth tensile specimens, mainly more angularity for the notched specimens. However, no gross changes were noted. The ratio of the strength of the samples tested in GH to the strength of samples tested in GHe remained near 1 which further indicates no hydrogen embrittlement occurred.

Stress rupture testing revealed one of the few differences in samples tested in H and He. Samples tested in high pressure GH had lower lives and reductions in area than those tested in high pressure GHe but were equivalent to the baseline uncharged specimens tested in vacuum. Given the longer time associated with the stress rupture test versus a tensile test, the probable cause of the differences between the GH and GHe results is hydrogen diffusion to the voids and the creation of an internal pressure within the sample. Unfortunately the needed analysis to confirm this hypothesis could not be conducted before the end of this task.

LCF testing shows that at total strain ranges greater than 1.2 percent the average values of the H charged GRCop-84 samples are less than the lower 95 percent confidence of the baseline GRCop-84. However, no differences such as grain boundary decohesion, cleavage fractures or hydrogen bubbles were noted on the fracture surfaces. Hydrogen atom-dislocation interactions and specimen design need to be examined to determine if either influences the LCF lives of charged specimens tested n GH and GHe. Scatter, especially at the 2 percent total strain range, may play a significant role in this observation which indicates additional testing would be beneficial.

While additional testing is warranted when the facilities become available, the results from this survey indicate that GRCop-84 does not suffer large reductions in properties or changes in fracture modes when exposed to high pressure hydrogen even under conditions which thermodynamics indicate could promote niobium hydride formation. This makes GRCop-84 generally suitable for use in a high pressure hydrogen environment.

References

1. W.H. Johnson, On Some Remarkable Changes Produced in Iron by the Action of Hydrogen and Acids, Proc. Roy. Soc., London, Vol. 23, (1874–1875), pp. 168–179.
2. K. Sadananda and R. Sreenivasan, Analysis of Fatigue Crack Growth Behavior in Niobium-Hydrogen Alloys Using the Unified Approach to Fatigue Damage, International Journal of Fatigue, Volume 23, Supplement 1, (2001), pp. 357–364.
3. J. Lufrano, P. Sofronis, and H.K. Birnbaum, Elastoplastically Accommodated Hydride Formation and Embrittlement, Journal of the Mechanics and Physics of Solids, Volume 46, Issue 9, (14 Sept. 1998), pp. 1497–1520.
4. D.T. Peterson, A.B. Hull and B.A. Loomis, Hydrogen Embrittlement Considerations in Nb-Base Alloys for Application in the ITER Diverter, Journal of Nuclear Materials, Volumes 191–194, Part 1, (Sept. 1992), pp. 430–432.
5. S. Gahr, M.L. Grossbeck, and H.K. Birnbaum, Hydrogen Embrittlement of Nb I – Macroscopic Behavior at Low Temperatures, Acta Metallurgica, Volume 25, Issue 2, (Feb. 1977), pp. 125–134.
6. M.L. Grossbeck and H.K. Birnbaum, Low Temperature Hydrogen Embrittlement of Niobium II – Microscopic Observations, Acta Metallurgica, Volume 25, Issue 2, (Feb. 1977), pp. 135–147.
7. S. Gahr and H.K. Birnbaum, Hydrogen Embrittlement of Niobium – III. High Temperature Behavior, Acta Metallurgica, Volume 26, Issue 11, (Nov. 1978), pp. 1781–1788.
8. Zielinski, Hydrogen-Assisted Degradation of Some Non-Ferrous Metals and Alloys, Journal of Materials Processing Technology, Volume 109, Issues 1–2, (1 Feb. 2001), pp. 206–214.
9. Y. Liang, P. Sofronis, and R. H. Dodds, Jr., Interaction of Hydrogen With Crack-Tip Plasticity: Effects of Constraint on Void Growth, Materials Science and Engineering A, Volume 366, Issue 2, (15 Feb. 2004), pp. 397–411.
10. M. Gao, D.J. Dwyer, and R.P. Wei, Niobium Enrichment and Environmental Enhancement of Creep Crack Growth in Nickel-Base Superalloys, Scripta Metallurgica et Materialia, Volume 32, Issue 8, (15 April 1995), pp. 1169–1174.
11. J.F. Smith, The H-Nb Phase Diagram, Bulletin of Alloy Phase Diagrams, Vol. 4. No. 1, (1983), pp. 39–46.
12. Ellis, David L.; Misra, Ajay K.; Dreshfield, Robert L. Effect of Hydrogen Exposure on a Cu-8 Cr-4 Nb Alloy, NASA-TM-106429, NASA Lewis Research Center, Cleveland, OH, (Dec. 1993).

13. M. Venkatraman and J.P. Neumann, The Cr-Nb (Chromium-Niobium) System, Bull. of Alloy Phase Diagrams, Vol. 7, No. 5, (1986), pp. 462–466.
14. D.L. Ellis, GRCop-84, Aerospace Structural Materials Handbook Supplement, CINDAS, Purdue University, West Lafayette, IN (Oct. 2001).
15. B.A. Lerch, Low Cycle Fatigue of GRCop-84, NASA TM, NASA Glenn Research Center, to be published.
16. W.A. Spitzig, D.T. Peterson and F.C. Laabs, Effect of Hydrogen on The Mechanical Properties of a Deformation Processed Cu-20% Nb Composite, J. of Matl. Sci., Vol. 26. (1991), pp. 2000–2006.
17. W.A. Spitzig, C.V. Owen, and T.E. Scott, Effects of Nitrogen on The Mechanical Behavior of Hydrogenated V, Nb, and Ta, Metall. Trans., Vol. 17A, (1986), pp. 527–535.
18. C.A. Michaluk, L.E. Huber, and R.B. Ford, Niobium and Niobium 1% Zirconium for High Pressure Sodium (HPS) Discharge Lamps, Niobium: Science and Technology, Proc. of the Intl. Symp. Niobium 2001, Orlando, FL, Dec. 2–5, 2001, Niobium 2001 Limited, Bridgeville, PA (2002), pp. 261–268.
19. K.S. Chan, The Fracture Toughness of Niobium-Based, In Situ Composites, Metallurgical and Materials Transactions A (Physical Metallurgy and Materials Science), Volume 27A, Issue 9, (1996), pp. 2518–2531.
20. D.L. Davidson, K.S. Chan, and D.L. Anton, The Effects on Fracture Toughness of Ductile-Phase Composition and Morphology in Nb-Cr-Ti And Nb-Si In Situ Composites, Metallurgical and Materials Transactions A (Physical Metallurgy and Materials Science), Volume 27A, Issue 10, (1996), pp. 3007–3018.
21. L.F. Coffin, Damage Processes In Time-Dependent Fatigue – A Review, Creep-Fatigue-Environment Interactions, R.M. Pelloux and N.S. Stoloff, Eds., TMS-AIME, Warrendale, PA, (1980), pp. 1–23.
22. D.N. Williams, The Hydrogen Embrittlement of Titanium Alloys, J. of the Inst. of Metals, Vol. 91, (1962–63), pp. 147–152.
23. C.A. Zapffe and C.E. Sims, Hydrogen Embrittlement, Internal Stress and Defects in Steels, Trans, of AIME, Vol. 145, (1941), pp. 225–261.

REPORT DOCUMENTATION PAGE

Form Approved
OMB No. 0704-0188

1. AGENCY USE ONLY (*Leave blank*)	2. REPORT DATE	3. REPORT TYPE AND DATES COVERED
	April 2006	Technical Memorandum

4. TITLE AND SUBTITLE

Effects of Hydrogen on GRCop-84

5. FUNDING NUMBERS

WBS–22–617–44–20

6. AUTHOR(S)

David L. Ellis and Keith Hastings

7. PERFORMING ORGANIZATION NAME(S) AND ADDRESS(ES)

National Aeronautics and Space Administration
John H. Glenn Research Center at Lewis Field
Cleveland, Ohio 44135–3191

8. PERFORMING ORGANIZATION REPORT NUMBER

E–15555

9. SPONSORING/MONITORING AGENCY NAME(S) AND ADDRESS(ES)

National Aeronautics and Space Administration
Washington, DC 20546–0001

10. SPONSORING/MONITORING AGENCY REPORT NUMBER

NASA TM—2006-214269

11. SUPPLEMENTARY NOTES

David L. Ellis, Glenn Research Center; Keith Hastings, ERC/Jacobs Sverdrup, Marshall Space Flight Center, Huntsville, Alabama 35812. Responsible person, David L. Ellis, organization code RXA, 216–433–8736.

12a. DISTRIBUTION/AVAILABILITY STATEMENT

Unclassified - Unlimited
Subject Category: 26

Available electronically at http://gltrs.grc.nasa.gov
This publication is available from the NASA Center for AeroSpace Information, 301–621–0390.

12b. DISTRIBUTION CODE

13. ABSTRACT ***(Maximum 200 words)***

This report is a section of the final report on the GRCop-84 task of the Constellation Program and incorporates the results obtained between October 2000 and September 2005 when the program ended. GRCop-84 contains approximately 5.5 wt% Nb. Nb can react with H and embrittle easily. Previous work had indicated the thermodynamic possibility that Cr_2Nb could react with H and form niobium hydrides in the presence of high pressure H such as seen in the Space Shuttle Main Engine. In this study, samples were charged with H and then tested in both high pressure H and He environments to determine if measurable differences existed which indicate that hydrogen embrittlement occurs in GRCop-84. Tensile, notched tensile, stress rupture and low cycle fatigue properties were surveyed. High pressure H environment stress rupture testing resulted in a lower reduction in area than a high pressure He environment, and the LCF lives at high strain ranges fall below the lower 95 percent confidence interval for the baseline data, but in general no significant differences were noted either between H and He environment tests or between hydrogen charged materials and the baseline, uncharged extruded GRCop-84 data sets. There was also no discernable evidence of the formation of hydrides or changes in fracture morphology indicating hydrogen embrittlement occurred.

14. SUBJECT TERMS	15. NUMBER OF PAGES
Hydrogen embrittlement; Copper alloys	29
	16. PRICE CODE

17. SECURITY CLASSIFICATION OF REPORT	18. SECURITY CLASSIFICATION OF THIS PAGE	19. SECURITY CLASSIFICATION OF ABSTRACT	20. LIMITATION OF ABSTRACT
Unclassified	Unclassified	Unclassified	